JOURNAL OF GEOPHYSICAL RESEARCH, VOL. 113, D14S12, doi:10.1029/2007JD009349, 2008

A satellite-based assessment of transpacific transport of pollution aerosol

Hongbin Yu,[1,2] Lorraine A. Remer,[2] Mian Chin,[2] Huisheng Bian,[1,2] Richard G. Kleidman,[2,3] and Thomas Diehl[1,2]

Received 4 September 2007; revised 23 November 2007; accepted 28 January 2008; published 22 April 2008.

[1] It has been well documented that pollution and dust from east Asia can be transported across the North Pacific basin, reaching North America and beyond. In this study, we assess the transpacific transport of "pollution aerosol" (defined as a mixture of aerosols from urban/industrial pollution and biomass burning) by taking advantage of the much improved measurement accuracy and enhanced new capabilities of satellite sensors in recent years. A 4-year (2002 to 2005) climatology of optical depth for pollution aerosol was generated from Moderate Resolution Imaging Spectroradiometer (MODIS) observations of fine- and coarse-mode aerosol optical depths. The pollution aerosol mass loading and fluxes were then calculated using measurements of the dependence of aerosol mass extinction efficiency on relative humidity and of aerosol vertical distributions from field campaigns and available satellite observations in the region. We estimated that about 18 Tg/a pollution aerosol is exported from east Asia to the northwestern Pacific Ocean, of which about 25% reaches the west coast of North America. The imported flux of 4.4 Tg/a to North America is equivalent to about 15% of local emissions from the United States and Canada. The pollution fluxes are largest in spring and smallest in summer. For the period we have examined the strongest export and import of pollution particulates occurred in 2003, largely because of record intense Eurasia boreal forest fires in spring and summer. The overall uncertainty of pollution fluxes is estimated at a factor of 2. Simulations by the Goddard Chemistry Aerosol Radiation and Transport (GOCART) and Global Modeling Initiative (GMI) models agree quite well with the satellite-based estimates of annual and latitude-integrated fluxes, with larger model-satellite differences in latitudinal and seasonal variations of fluxes.

Citation: Yu, H., L. A. Remer, M. Chin, H. Bian, R. G. Kleidman, and T. Diehl (2008), A satellite-based assessment of transpacific transport of pollution aerosol, *J. Geophys. Res.*, *113*, D14S12, doi:10.1029/2007JD009349.

1. Introduction

1.1. Asian Pollution and Intercontinental Transport

[2] East Asia is an important source region of a variety of natural and anthropogenic aerosols, also called particulate matter (PM). China, the world's most populous country has been undergoing persistent rapid industrialization and urbanization and the burgeoning expansion of automobile usage over the last two decades. As a result, China has more than doubled its emissions in recent decades to quickly become one of the largest emitters of aerosols and aerosol precursors in the world [*Bond et al.*, 2004; *Richter et al.*, 2005; *Wang et al.*, 2006; *Akimoto et al.*, 2006]. The large emissions of aerosols in east Asia may have brought about substantial impacts to climate [*Huang et al.*, 2006], hydrological cycle [*Menon et al.*, 2002], solar radiation reaching the surface [*Qian et al.*, 2007], crop yields [*Chameides et al.*, 1999], and human health [*Xu et al.*, 1998] in the region.

[3] The east Asian aerosols could also impose far-reaching environmental impacts at continental, hemispherical and even global scales, because of long-range transport. East Asia is one of the main warm conveyor belts (WCB) inflow regions, where airstreams rapidly transport the atmospheric boundary layer (ABL) air into the upper troposphere (UT) [*Stohl*, 2001; *Eckhardt et al.*, 2004]. The ABL pollution can also be lifted to the UT by frontal and postfrontal convection, orographic lifting, and the ABL turbulent mixing. As a result, emissions from Asia can experience rapid vertical transport [*Stohl et al.*, 2002]. Pollutants lifted to the free troposphere travel initially poleward and eastward by midlatitude storm tracks, turn toward the equator thereafter, and then reach mainly the middle and upper troposphere of the northeastern Pacific. Such high-level transpacific transport takes about a week [*Holzer et al.*, 2005]. The polluted Asian air over the northeastern Pacific can then be transported downward to influence the North American ABL through subsidence associated with subtropical Pacific highs

[1] Goddard Earth Science and Technology Center, University of Maryland at Baltimore County, Baltimore, Maryland, USA.
[2] Laboratory for Atmospheres, NASA Goddard Space Flight Center, Greenbelt, Maryland, USA.
[3] Science System and Applications, Inc., Lanham, Maryland, USA.

0148-0227/08/2007JD009349$09.00

[*Heald et al.*, 2003] and through mesoscale mountain circulations in western North America [*McKendry et al.*, 2001]. Air pollutants can also be transported across the North Pacific at low altitudes with a relatively low rate through ABL outflow associated with cold fronts [*Liang et al.*, 2004; *Liu et al.*, 2003; *Holzer et al.*, 2005].

[4] There has been mounting evidence for intercontinental and even hemispheric transport as provided by long-term surface monitoring networks, in situ measurements from intensive field campaigns, and satellite observations backed by model simulations. Dust storms and industrial emissions have long been observed to influence the North Pacific [*Duce et al.*, 1980], to contribute to particulate matter level on the western boundary of North America [*Andreae et al.*, 1988; *Jaffe et al.*, 1999, 2005; *Husar et al.*, 2001; *Wilkening et al.*, 2000; *McKendry et al.*, 2001] and on the East Coast after traversing the continent [*Biscaye et al.*, 2000; *VanCuren and Cahill*, 2002], and to even affect Europe [*Stohl et al.*, 2007; *Grousset et al.*, 2003]. Model simulations also suggest substantial transpacific transport of aerosols [*Chin et al.*, 2004, 2007; *Heald et al.*, 2006; *Hadley et al.*, 2007].

[5] The regional and global impacts of Asian aerosols are largely unknown but the implications are quite powerful [*Stohl et al.*, 2002]. Because particulates with a diameter less than 2.5 μm (PM2.5), can cause cardiovascular and respiratory diseases, increasingly stringent standards for PM2.5 have been enforced by the U.S. Environmental Protection Agency (EPA). While most pollution sources are local, the transboundary and intercontinental transport of PM2.5 from Asia may compromise efforts of some western U.S. states to attain air quality goals through domestic and regional emission controls [e.g., *Heald et al.*, 2006; *Chin et al.*, 2007; *Fairlie et al.*, 2007]. Aerosols can perturb the radiative budget of the earth-atmosphere system directly through scattering and absorbing radiation and indirectly through altering cloud formation and cloud properties. The deposition of soot in snow and ice can also reduce surface reflectance and hence perturb the surface energy budget [*Hansen and Nazarenko*, 2004]. Linked through these processes, aerosols can thereby affect atmospheric circulations and precipitation. It has been suggested that an increase of particulate air pollution may reduce orographic precipitation in the mountain ranges of the western United States [*Rosenfeld and Givati*, 2006; *Jirak and Cotton*, 2006], causing a significant shortage of water resources in the western states. Asian dust particles have been observed to affect the formation of clouds over the western United States [*Sassen*, 2002]. A satellite-detected intensification of the North Pacific midlatitude storm tracks has been associated with an increase of aerosol emission in Asia in the last two decades [*Zhang et al.*, 2007]. This suggests a possible feedback influence of long-range transport of aerosols, because the North Pacific storm tracks effectively transport pollution and dust from east Asia to North America.

1.2. A Satellite Perspective

[6] A better understanding of aerosol transport, transformation, and distribution is required to assess a variety of aerosol impacts on a wide range of scales and formulate an effective strategy for combating air pollution. Because of the large emissions and rate of increase in Asia, the potential impacts on the environment are relatively easy to detect and can be studied over a large dynamic range. As such, in the past two decades, the aerosol related scientific and environmental issues in the North Pacific basin have been a focus of several large-scale international experiments [e.g., *Huebert et al.*, 2003; *Jacob et al.*, 2003; *Bertschi et al.*, 2004; *Parrish et al.*, 2004]. These missions with the implementation of coordinated and multiplatform observation strategies have been providing comprehensive snapshots of regional aerosols. For all of their advantages, field campaigns are inherently limited by their relatively short duration and small spatial coverage. Therefore they alone are not adequate to assess the temporal and spatial variations of transpacific transport of aerosols.

[7] Satellite remote sensing of aerosols can augment these missions by expanding temporal and spatial scales to generate measurement based estimates of aerosol intercontinental transport. In addition, these estimates can be used to evaluate model simulations. Satellite imagers have been providing a wealth of evidence for intercontinental and hemispheric transport of aerosols in a qualitative or semiquantitative manner for nearly three decades [e.g., *Lyons et al.*, 1978; *Chung*, 1986; *Herman et al.*, 1997]. Quantitative estimates of aerosol mass and transport were also attempted decades ago [*Fraser*, 1976; *Fraser et al.*, 1984]. However, these early estimates were subject to large uncertainties because of poor accuracy of early satellite measurements. Quantitative assessments of aerosol intercontinental transport became feasible only recently as a result of the much improved measurement accuracy and enhanced new capabilities of satellite sensors [*King et al.*, 1999; *Kaufman et al.*, 2002], as well as a constellation of multiple satellites (such as "A-Train") with complementary measurement capabilities. Although current and near-future satellite sensors cannot directly measure aerosol composition, measurements can be used to categorize aerosol types in terms of particle size (i.e., fine versus coarse), shape (i.e., spherical versus nonspherical), and absorption (i.e., scattering versus absorbing) because of implementation of multiwavelength, multiangle, and polarization measurements [*Higurashi and Nakajima*, 2002; *Tanré et al.*, 2001]. Algorithms have been recently developed to quantitatively estimate the optical depth of pollution aerosol and dust [e.g., *Kaufman et al.*, 2005a, 2005b]. The new capabilities associated with passive sensors are being further enhanced by emerging lidar measurements in recent years that are providing essential information of aerosol vertical distributions [*Spinhirne et al.*, 2005; *Winker et al.*, 2003]. It is currently feasible to develop a satellite-based approach supplemented by in situ measurements and model simulations to quantify aerosol intercontinental transport.

[8] In this study we make our first attempt at this approach by estimating the mass fluxes of pollution aerosol exported from east Asia to the North Pacific basin and imported to North America on the basis of satellite data. For this purpose, the satellite observed aerosol is categorized into three generic types on the basis of its sources, i.e., maritime aerosol, mineral dust, and pollution aerosol. Here "pollution aerosol" is considered to be a mixture of aerosols from urban/industrial pollution and biomass burning, which is predominately in submicron size or fine mode. All biomass burning is assumed to be man made here. Note that this definition may be different from that in other

studies, as dust is sometimes called pollution. The method takes advantage of the Moderate resolution Imaging Spectroradiometer (MODIS) high-accuracy measurements of aerosol optical depths over ocean, fine and coarse mode separately, in combination with satellite measurements of aerosol vertical profiles from the Geoscience Laser Altimeter System (GLAS), and in situ measurements of comprehensive aerosol chemistry and physics from intensive field campaigns in the regions. The estimated aerosol import and export fluxes are compared with the Goddard Chemistry Aerosol Radiation Transport (GOCART) and Global Modeling Initiative (GMI) simulations. The satellite observations of aerosol and aerosol models are described in section 2. In section 3, an approach to deriving pollution aerosol fluxes from satellites is presented. Seasonal and interannual variations of the satellite-estimated export and import of pollution aerosol are discussed and compared with the model simulations in section 4. Uncertainties associated with the flux estimate and potential of reducing uncertainties by integrating the Cloud-Aerosol Lidar with Orthogonal Polarization (CALIOP) and other A-Train observations are also discussed. Major results are summarized in section 5.

2. Description of Aerosol Data and Models

2.1. MODIS Aerosol Optical Depths

[9] MODIS aboard both Terra and Aqua is making near global daily observations of atmospheric aerosols since February 2000 (Terra) and July 2002 (Aqua). MODIS uses seven wavelength channels (between 0.47 and 2.13 μm) to retrieve aerosol properties over cloud and surface-screened areas. Separate algorithms are implemented over land and ocean [*Kaufman et al.*, 1997; *Tanré et al.*, 1997; *Remer et al.*, 2005; *Levy et al.*, 2007]. MODIS products are widely used by the community for a variety of purposes, including descriptions of the regional, seasonal and global distribution of aerosols and their relationship to other pollutants [*Yu et al.*, 2003; *Chin et al.*, 2004], studies of the effect of aerosol on atmospheric chemistry and local air pollution [*Engel-Cox et al.*, 2004; *Al-Saadi et al.*, 2005], measurements of the aerosol radiative forcing of climate [*Yu et al.*, 2004; *Remer and Kaufman*, 2006], studies of the aerosol interaction with the meteorological field and with clouds [*Koren et al.*, 2004; *Kaufman et al.*, 2005d], and synergy with other sensors to enhance standard MODIS retrievals and offer new standalone products [*Kaufman et al.*, 2003a, 2003b; *León et al.*, 2003].

[10] Because of its wide spectral range over ocean, MODIS has the unique capability to retrieve not only spectral aerosol optical depth (τ) at seven wavelengths from 0.47 to 2.13 μm with great accuracy, i.e., $\pm 0.03 \pm 0.05\tau$ [*Remer et al.*, 2002, 2005], but also the quantitative aerosol size parameters (e.g., effective radius and fine-mode fraction) [*Kaufman et al.*, 2002; *Remer et al.*, 2005; *Kleidman et al.*, 2005]. The fine-mode fraction (FMF) is a measure of the contribution of fine-mode or submicron aerosols to the optical depth. Because anthropogenic aerosols are predominately in submicron range, FMF can be used as a tool for separating anthropogenic aerosol from dust, as demonstrated in some previous studies. *Kaufman et al.* [2005a] developed an algorithm that uses MODIS/Terra aerosol optical depth (AOD) and FMF to distinguish dust from pollution and maritime aerosols and evaluate the column concentration, transport and deposition of dust over the Atlantic Ocean. The results confirm seasonal variations of magnitude and location of African dust transport across the Atlantic Ocean. In particular, the estimated deposition of 50 Tg dust in the Amazon, much larger than previous estimates, may explain the paradox between the need of nutrition by the Amazon forest and the source of the nutrition. A similar algorithm has been employed to estimate anthropogenic and natural components of aerosols [*Kaufman et al.*, 2005b], which has since inspired the community to further explore the use of satellites to quantify aerosol radiative forcing by anthropogenic aerosol [e.g., *Anderson et al.*, 2005, *Bellouin et al.*, 2005; *Christopher et al.*, 2006; *Yu et al.*, 2006].

2.2. GOCART and GMI Aerosol Simulations

[11] The global model GOCART is driven by assimilated meteorological fields from the Goddard Earth Observing System Data Assimilation System (*GEOS DAS*) [*Chin et al.*, 2002]. GOCART simulates the major aerosol types: sulfate, dust, black carbon (BC), organic carbon (OC), and sea salt. Emissions from anthropogenic, biomass burning, biogenic, and volcanic sources and wind-blown dust and sea salt are included in the model. Processes represented in GOCART are chemistry, convection, advection, boundary layer mixing, dry and wet deposition, gravitational settling, and hygroscopic growth of aerosol particles. The size distributions for individual components are prescribed and coagulation and condensation processes are not considered. Individual components don't interact with each other. Details of GOCART and evaluation of its results against observations are documented in a number of publications [e.g., *Chin et al.*, 2000a, 2000b, 2002, 2004; *Ginoux et al.*, 2001, 2004].

[12] The Global Modeling Initiative (GMI) aerosol module, adapted from the University of Michigan/LLNL IMPACT model [*Liu et al.*, 2007], is similar to the GOCART model in such aspects as fossil fuel emissions of SO_2, BC, and OC, and the advection core. On the other hand, the two models differ in aqueous phase reactions, dry and wet deposition, gravitational settling, and convective transport, among others. As such GOCART and GMI simulated mass concentration and flux of pollution aerosol can be different both in the horizontal and vertical, though both models are driven by the same meteorological fields from GEOS-4 in this study.

[13] For this study, we run each model twice, one with all aerosol sources and the other without anthropogenic and biomass burning sources. A difference between the two runs is used as a proxy for the pollution aerosol. Here we assume that biomass burning aerosols are fully man-made, which is somewhat consistent with the proxy assumption made for the MODIS estimate. Model calculated sulfate mass is converted to that of ammonium sulfate $(NH_4)_2SO_4$ for calculating pollution fluxes.

3. Approaches to Estimating Pollution Aerosol Fluxes From Satellites

[14] In this study we extend the method and analysis used by *Kaufman et al.* [2005a, 2005b] to estimate fluxes of pollution aerosol exported from east Asia and imported to

North America. A three-step method integrates data sets from multiple satellite sensors and in situ measurements from field campaigns to generate a 4-year (2002–2005) climatology of transpacific transport of pollution aerosol, as discussed in the following.

3.1. Deriving Optical Depth for Pollution Aerosol From MODIS Retrievals

[15] We use the method developed by *Kaufman et al.* [2005a, 2005b] to derive optical depth for pollution aerosol (τ_p) according to:

$$\tau_p = \frac{(f - f_d)\tau - (f_m - f_d)\tau_m}{(f_p - f_d)} \quad (1)$$

where τ and f represents aerosol optical depth and fine-mode fraction respectively, both at 550 nm. Subscripts p, d, and m denote pollution, dust, and maritime aerosol, respectively. Here we assume that optical depth for volcanic and biogenic aerosols is negligible. Such assumptions may bias our estimate of pollution optical depth to a high value especially in years following major volcano eruptions. We apply the method to Collection 4, Level 3 daily MODIS/Terra aerosol data (at $1^\circ \times 1^\circ$ resolution) from which empirical coefficients in (1), f_m, f_d, f_p, and τ_m were derived by *Kaufman et al.* [2005a, 2005b].

[16] We modify the method developed by *Kaufman et al.* [2005a, 2005b] by taking into account the seasonal and spatial variations of fine-mode fraction for maritime aerosol (f_m). Over remote oceans, boundary layer aerosols consist of sea salt particle generated from bursting bubbles, sulfate from oxidation of dimethyl sulfide (DMS), and organic matter. While sulfate from DMS oxidation and organic particles are in the submicron size range, the sea salt aerosols have much broader size distributions [*Bates et al.*, 2001] and the fine-mode sea salt is a significant contributor to sea salt optical depth and also an important component of fine-mode maritime aerosol optical depth. These marine-generated fine-mode aerosols should depend on a variety of atmospheric and oceanic parameters, such as ocean color, sea surface temperature (SST), near-surface wind speed, and atmospheric oxidizing capacity. This complexity gives rise to large seasonal and geographical variations in the maritime FMF (ranging from 0.2 to 0.8), as evidenced consistently in a MODIS-derived proxy for maritime aerosol (e.g., AOD less than 0.1), and GOCART and GMI simulations of purely maritime aerosol (H. Yu et al., Variability of maritime aerosol fine-mode fraction and estimates of anthropogenic aerosol component from MODIS, manuscript in preparation, 2008), as well as aircraft measurements [*Shinozuka et al.*, 2004]. A use of the seasonally and geographically varying maritime FMF decreases the pollution aerosol optical depth by as much as 30% in coastal areas of the North Pacific and in summer, in comparison to that using the constant f_m [*Kaufman et al.*, 2005a, 2005b].

3.2. Determining Major Transport Heights of Pollution Aerosol

[17] To transform aerosol optical depth to aerosol mass loading and flux, major transport heights of pollution aerosol are needed to determine the relative humidity and wind speed representative of satellite observed pollution plumes. Passive sensors like MODIS acquire columnar aerosol properties which give essentially no information on vertical distributions of aerosol. In this study we determine the transport heights of pollution aerosol on the basis of aircraft measurements in the region, available surface and satellite lidar observations, and model simulations.

[18] Observations over the northwestern Pacific during several field campaigns indicate multiple pollution layers from the surface up to the middle troposphere with a significant fraction of pollution aerosol mass above the ABL [e.g., *Bahreini et al.*, 2003]. For example, $SO_4^=$ and NH_4^+ profiles over the northwestern Pacific indicate that about one third of sulfate mass is above 2 km [*Dibb et al.*, 2003; *Chin et al.*, 2003]. Carbonaceous aerosols were even more concentrated than sulfate in the upper troposphere [*Huebert et al.*, 2004]. A global 3-D chemical transport model showed that the transpacific transport of Asian anthropogenic aerosols takes place mainly in 900–700 hPa layer because of scavenging during transport either in the boundary layer or during lifting to the upper troposphere [*Heald et al.*, 2006]. Measurements over the northeastern Pacific Ocean and western North America indicate persistent Asian continental influences in the lower free troposphere [*VanCuren et al.*, 2005]. While Siberian boreal fire emissions and Asian dusts tend to elevate the aerosol extinction mainly above the ABL (from 2 to 3 km up to 6 km) over the northeastern Pacific, the enhancement of aerosol extinction in the ABL results largely from transport of industrial pollution aerosol [*Bertschi et al.*, 2004; *Price et al.*, 2003; *de Gouw et al.*, 2004]. Air masses from Southeast Asia and China are generally observed at higher altitudes than air from Japan and Korea [*de Gouw et al.*, 2004]. A tracer model simulation suggests that Asian pollution transported to the west coast of the northwestern United States is largely confined to the lowest 3 km layer, whereas the isentropic trajectory indicates a somewhat higher transport height [*Jaffe et al.*, 1999].

[19] Multiyear measurements from the ground-based micropulse lidars in the Korean peninsula [*Kim et al.*, 2007] indicate that, on an annual basis, roughly 2/3 of columnar AOD is contributed by aerosols below 2 km. In comparison to summer and fall measurements, aerosol extinction in spring and winter is enhanced above the boundary layer and below about 6 km, which is presumably attributable to seasonal variations of Asian dust storms. Lidar measurements over Japan and Korea during the Aerosol Characterization Experiment (ACE) -Asia give the similar vertical distribution for polluted cases [*Quinn et al.*, 2004]. Observations of aerosol profiles from GLAS are also examined for two available periods. Figure 1 shows profiles of the frequency and average backscatter of GLAS detected aerosol layers during September–November 2003 (Figure 1b) and February–March 2004 (Figure 1c) in four coastal regions as illustrated in Figure 1a. While aerosol layers are largely detected in the boundary layer in both periods and all regions, some enhanced layers with backscatter comparable to that in the ABL are indeed detected in the free atmosphere. Such enhancement in the free atmosphere is more pronounced in February–March than in September–November, presumably because of more frequent dust plumes in late winter and spring that are generally transported at higher altitudes than pollution plumes. Note also that the detected aerosol in

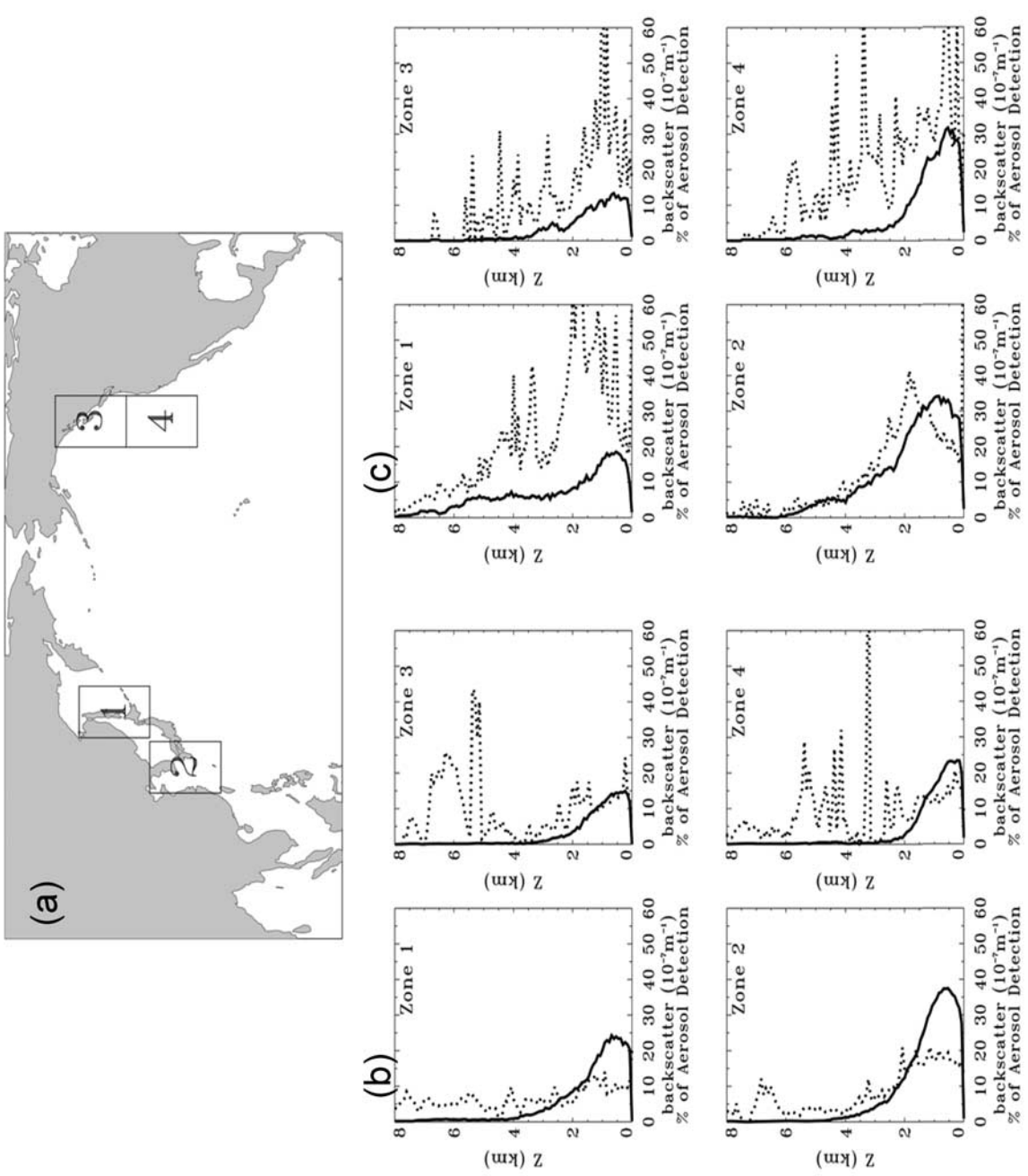

Figure 1. (a) Illustration of four boxes into which GLAS data are aggregated for deriving average profiles of aerosol backscatter and detection frequency. (b) Profiles of GLAS aerosol detection frequency (solid line) and average backscatter (dotted line) for 25 September to 19 November 2003 calculated in four boxes as defined in Figure 1a. (c) Same as Figure 1b, but for 17 February to 4 March 2004.

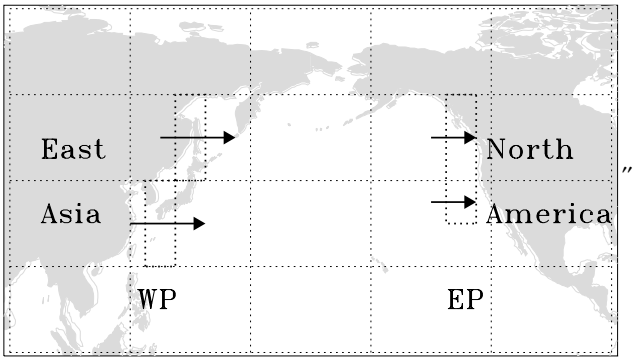

Figure 2. Schematic of calculating pollution mass fluxes across meridional planes with a width of 10° in longitude in the West Pacific (WP) and East Pacific (EP). The latitudinal integration over WP and EP is used to represent east Asia outflow and North America inflow, respectively.

the ABL could also be partially attributable to the maritime aerosol. It is thus difficult to characterize pollution aerosol from only GLAS aerosol measurements.

[20] To be consistent with the observations and models discussed above, we assume that the aerosol optical depth in each of three layers, namely 0–1 km, 1–2 km, and above 2 km (denoted respectively as L1, L2, and L3), accounts for one third of the columnar pollution AOD. That is, 67% of pollution AOD is assume to reside in the lowest 2 km layer (approximately, ABL) and 33% above the ABL. This is a simplified representation for the complicated layering structure of aerosols in reality. Seasonal, interannual, and geographical variations of pollution transport heights are not considered in this study because of the paucity of available observations. Therefore seasonal, interannual, and geographical variations of pollution aerosol fluxes discussed in this study result from a combination of the MODIS observed variations of column aerosol mass loading and variations of wind and humidity profiles.

3.3. Calculating Mass Loading and Flux of Pollution Aerosol

[21] Pollution aerosol optical depth (τ_p) derived above is for hydrated pollution aerosol in ambient conditions measured by MODIS. In each layer (l), τ_p can be converted to dry mass loading M_p as follows:

$$M_p(l) = \frac{\tau_p(l)}{f[RH(l)]MEE_p} \tag{2}$$

where MEE_p (m^2g^{-1}) is dry mass extinction efficiency of pollution aerosol; and f(RH) is a function that accounts for an increase of aerosol extinction with increasing relative humidity (RH), depending on chemical composition with monotonic (smoothly varying) or deliquescent (step change) growth [*Quinn et al.*, 2005; *Carrico et al.*, 2003]. For MEE_p we use a value of 4 m^2g^{-1} based on measurements during ACE-Asia campaign for continental outflows with weak dust influence and at low RH [*Bates et al.*, 2006, and references therein]. For f(RH) we use an empirical function that is an average of the monotonic and deliquescent growth curves observed during ACE-Asia for pollution aerosol [*Carrico et al.*, 2003]. Measurements of RH from the Atmospheric Infrared Sounder (AIRS) [*Aumann et al.*, 2003] are used as input to quantify the hygroscopic growth of aerosols and convert the measured optical depth in ambient conditions to the (dry) mass loading. To comply with vertical resolution of AIRS data sets, we use RH at 925, 850, and 700 hPa to derive pollution mass loading in L1, L2, and L3 layer, respectively.

[22] The daily mass loading (gm^{-2}) for pollution aerosol derived at individual 1° × 1° grids is aggregated to the monthly average (M_p) over the flux calculation boxes. Then monthly average zonal winds at 925, 850, and 700 hPa from the Goddard Earth Observing System Data Assimilation System (GEOS DAS) with current version of GEOS-4 are used to calculate pollution fluxes (gs^{-1}) in L1, L2, and L3 layer, respectively. For a segment with a length of L (m) that is parallel to longitudes, we use east-west wind component U to calculate the columnar fluxes as follows:

$$F_p = \sum_{l=1}^{3} M_p(l)U(l)*L \tag{3}$$

The calculated monthly fluxes are aggregated into seasons and 10° latitude sections for analysis in the next section. As discussed later, a use of monthly averaged aerosol and wind field should not introduce significant uncertainties to the estimated pollution fluxes in the region.

4. Results and Discussion

[24] We applied the method discussed in section 3 to MODIS/Terra Level 3 daily 1° × 1° data from 2002 to 2005 to estimate fluxes of pollution aerosol exported from east Asia to West Pacific (WP) and imported to the West Coast of North America over East Pacific (EP). The flux estimation was done across meridional planes with a width of 10° in longitude, as illustrated in Figure 2. Over West Pacific, the meridional plane is centered at 130°E south of 40°N and at 140°E north of 40°N. On the other side of Pacific, the meridional plane is centered at 130°W. We integrate the calculated flux from 20°N to 60°N over WP to represent the east Asia outflow. Given that the transpacific transport usually shifts poleward after leaving east Asia and the transport in subtropical (20–30°N) EP is predominately controlled by easterlies, fluxes are integrated from 30°N to 60°N over EP to represent North America inflow. In the following, seasonal and latitudinal variations of MODIS-estimated export and import fluxes are discussed and compared with GOCART and GMI simulations in section 4.1. Interannual variability of pollution fluxes are examined for 2002–2005 period in section 4.2. In section 4.3, uncertainties associated with flux calculations are estimated and a potential of reducing the uncertainty is discussed in terms of integrating A-Train observations.

4.1. Seasonal and Latitudinal Variations of Pollution Fluxes

[25] Since most field experiments and promoted modeling studies of aerosols have been focusing on late winter and spring [e.g., *Tan et al.*, 2002; *Chin et al.*, 2004; *Heald et al.*, 2006; *Hadley et al.*, 2007], seasonal variations of

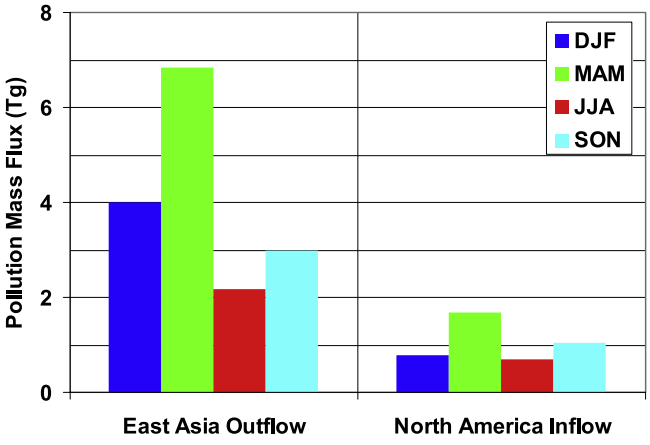

Figure 3. Seasonal variations of MODIS-derived east Asia outflow and North America inflow of pollution aerosol for 2004.

transpacific transport of pollution aerosol are not well understood. Figure 3 shows the MODIS-estimated seasonal pollution fluxes for 2004. Clearly, both east Asia outflow and North America inflow peaked in spring, with the flux of 6.8 and 1.7 Tg/season, respectively. The outflow and inflow are weakest but not negligible in summer, with a magnitude of about 1/3 of the springtime maximum and 10% of the annual flux. Winter and autumn appear to be transitional seasons when pollution fluxes are in between the springtime maximum and the summertime minimum. Over the western Pacific, the wintertime pollution flux is about 30% higher than that in autumn. Such seasonal variation for pollution aerosol fluxes is similar to simulations of carbon monoxide [*Liu et al.*, 2003].

[26] The observed seasonal variations of pollution aerosol fluxes are determined by a combination of meteorological conditions, emissions, chemistry and removal processes. In east Asia, emissions of pollution aerosol*s* and their precursors have some seasonal variations. In winter the use of coal in northern China is more than those in other seasons because of heating demands in winter. On the other hand, the production of sulfate aerosol from the combustion generated SO_2 is slower in the winter because of lower oxidant levels and slower reaction rates. Biomass burning shows strong seasonal variations; in south and Southeast Asia, the burning occurs mainly in spring, while in high-latitude Eurasian region, the burning peaks in spring and summer [e.g., *Giglio et al.*, 2006; *Bian et al.*, 2007]. Presumably the Asian monsoon system would play a much larger role in regulating the seasonality of transpacific transport, as suggested by a number of previous studies. The WCBs are stronger and occur more frequently in winter and spring [*Eckhardt et al.*, 2004] and the springtime dry convection can also be an important lifting mechanism over China [*Dickerson et al.*, 2007]. This in combination with strongest midlatitude westerlies results in the strongest pollutant transport in spring. The weakest pollutant transport in summer is a result of an offset of the westward transport by the eastward transport, particularly south of 30°N and the largest aerosol removal associated with summer monsoon circulation [*Holzer et al.*, 2005].

[27] On an annual basis, the MODIS-estimated pollution outflow and inflow is 16.0 and 4.2 Tg/a, respectively (Table 1). This suggests that about a quarter of east Asia outflow of pollution aerosol can reach the west coast of North America, if there is no additional contribution of pollution aerosol from elsewhere during transpacific transport. While this would be a reasonable assumption on an annual basis, the assumption may overestimate Asia's contribution to North America in summer season and certain years because of potential contributions of biomass burning smoke from Alaska. The smoke from Mexico and Central America in spring is unlikely to contribute significantly to the calculated North America inflow over 30–60°N. The MODIS estimate of 16 Tg outflow is slightly smaller than the GOCART simulation of 16.7 Tg, but about 10% larger than the GMI simulations of 14.2 Tg. For the North America inflow GOCART and GMI simulation respectively gives 5.3 Tg and 4.5 Tg, which is about 25% and 7% larger than the MODIS estimate of 4.2 Tg. The model simulations suggest that about one third of east Asia outflow can reach the west coast of North America, which is somewhat larger than the MODIS-based estimate. Figure 4 shows that on a seasonal basis satellite estimated and model simulated outflow and

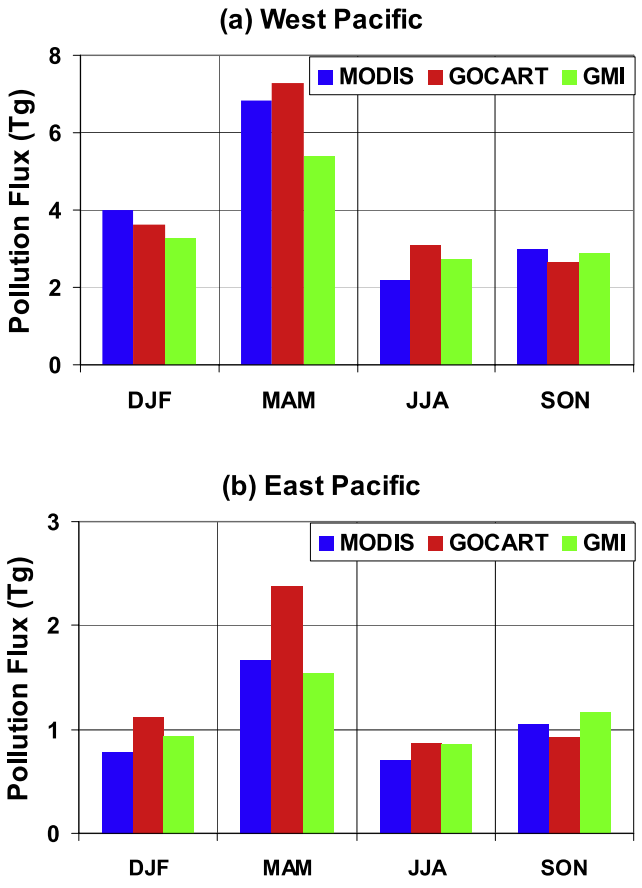

Figure 4. Comparisons of seasonal variations of meridional integrated pollution flux across the (a) West Pacific and (b) East Pacific for 2004.

Table 1. Comparisons of MODIS-Based Estimate and GOCART and GMI Simulations of East Asia Outflow and North America Inflow of Pollution Aerosol for 2004

Approach	East Asia Outflow, Tg/a	North America Inflow, Tg/a	Inflow/Outflow, %
MODIS	16.0	4.2	26
GOCART	16.7	5.3	32
GMI	14.2	4.5	31

inflow fluxes are still in reasonably good agreement. The largest satellite-model differences occurred in spring for both the east Asia outflow (with GMI flux smaller than the MODIS estimate by about 1.4 Tg or 40%) and the North America inflow (with GOCART flux larger than the MODIS estimate by 0.7 Tg or 40%).

[28] Meridional variations of annual pollution aerosol fluxes are compared between satellite estimate and model simulations, as shown in Figure 5. For east Asia outflow, MODIS estimated the maximum flux of 7.6 Tg/a in the 30–40°N segment, followed by 5.7 Tg/a in the 40–50°N segment. The flux integrated over the 30–50°N segment accounts for about 80% of the total east Asia outflow. A remaining 20% of the outflow is nearly evenly distributed in the 20–30°N and 50–60°N segments. For comparison, GOCART and GMI simulations give more or less the same flux in the 30–40°N segment as that in the 40–50°N segment. In the 30–40°N segment, the model simulations are smaller than the corresponding MODIS estimate by 20–30%. On the other hand, both model simulations are larger than the MODIS estimate by about 70% in the 20–30°N segment.

[29] For the North America inflow, MODIS estimates the highest flux of 1.8 Tg/a in the 40–50°N segment, followed by 1.4 Tg/a in the 50–60°N segment and 1.1 Tg/a in the 30–40°N segment. This suggests a general poleward shift of pollution plume during the transpacific transport. While GOCART fluxes are higher in the 30–60°N segments than the MODIS estimates, GMI flux is closer to the MODIS-based estimates. In the 20–30°N subtropical segment both GOCART and GMI give a nearly zero flux, while the MODIS-based estimate suggests a westward transport of pollution from North America (i.e., negative flux).This difference is likely to result from different transport heights assumed in the MODIS estimate and simulated by the models in conjunction with the shift of westerly boundary layer winds to easterlies in the free troposphere. The use of monthly average aerosol and wind in the MODIS estimate seemingly can introduce a large uncertainty in this region, as suggested by our sensitivity tests with GMI simulations.

[30] The above analysis suggests that in 2004 about 16 Tg pollution aerosol was exported from east Asia to the northwestern Pacific Ocean through mainly the 30–50°N segment. The pollution flux was largest in spring and smallest in summer. The summer flux was about 30% of the springtime flux. About one quarter of the pollution export from Asia may have reached the west coast of North America in that year. This substantial transpacific transport of pollution is arguably largely originating from Asia, but with nonnegligible contributions from Europe, Africa, and elsewhere depending on season and location [*Newell and Evans*, 2000; *Chin et al.*, 2007]. The satellite-based estimates agree with GOCART and GMI simulations remarkably well over broad meridional segments and on an annual basis. The comparisons also show reasonably good agreements over 10° meridional segments and on a seasonal basis.

4.2. Interannual Variability of Pollution Aerosol Fluxes

[31] While some interannual variations or trends of industrial emissions in east Asia have been suggested [e.g., *Carmichael et al.*, 2002; *Richter et al.*, 2005], biomass burning emissions that are controlled by meteorological and biospheric conditions as well as human activities are likely to show much larger interannual variations [*Duncan et al.*, 2003]. On the other hand, the interannual variability of Asian outflow resulting from large-scale variations in atmospheric circulation is the lowest, in comparison to other regions [*Liu et al.*, 2005]. It is thus expected that pollution fluxes exported from east Asia and imported to North America would show some interannual variations resulting mainly from variations in biomass burning smoke from Eurasia.

[32] We have applied the method to MODIS/Terra data for other years and derived the 4-year climatology (2002–2005) of pollution fluxes exported to the West Pacific and imported to the East Pacific. Figure 6 shows interannual variations of pollution aerosol optical depth in MAM and JJA. In MAM and JJA, 2003, the aerosol optical depth in the high-latitude North Pacific (40–60°N) was elevated to a

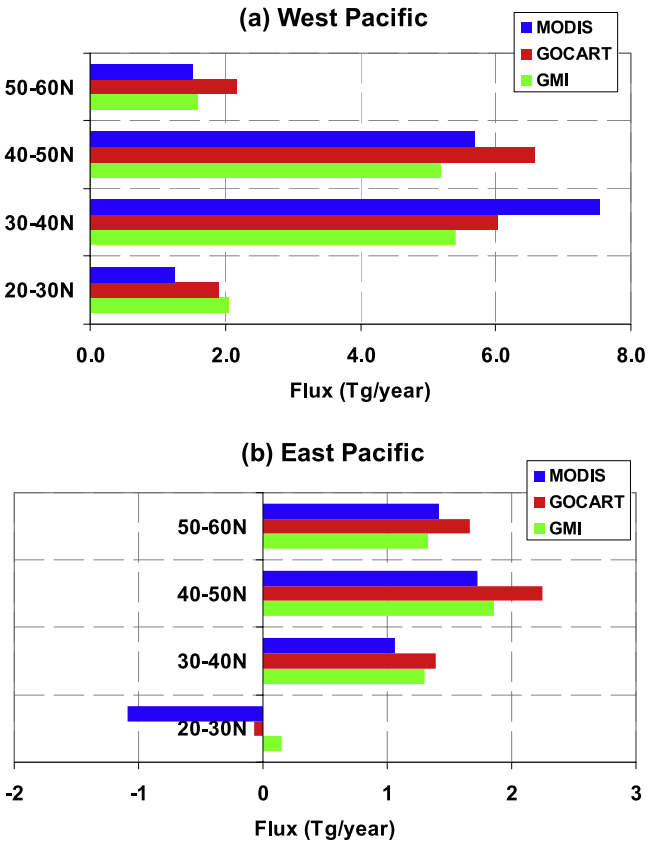

Figure 5. Comparisons of meridional variations of annual pollution flux for 2004 across the (a) West Pacific and (b) East Pacific.

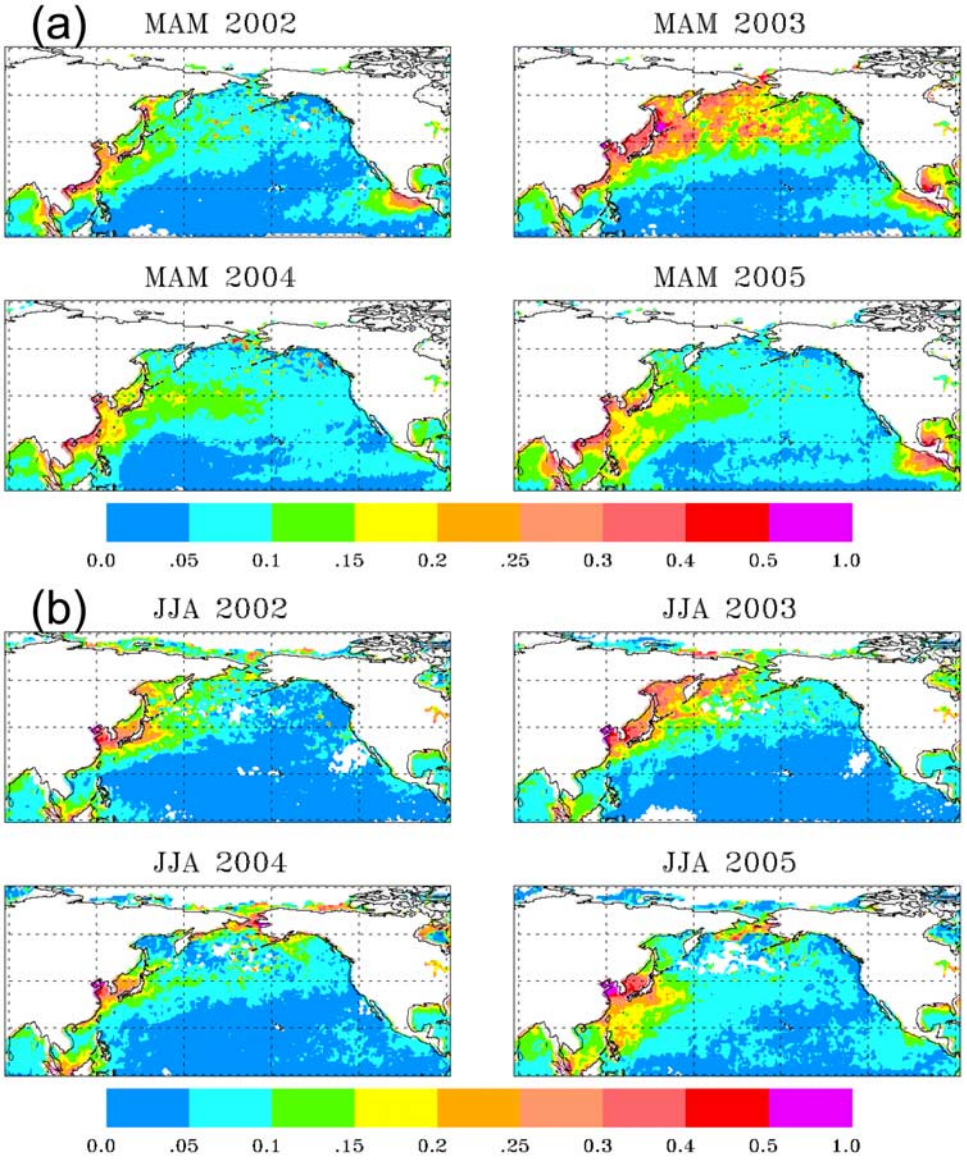

Figure 6. Interannual variations of pollution aerosol optical depth at 550 nm for (a) MAM, and (b) JJA derived from MODIS.

level that is more than a factor of 2 larger than in other years. This is corroborated with elevated TOMS absorbing aerosol index that suggests intense biomass burning smoke (not shown). In 2003, biomass fires burned a large area of south and east Russia, starting from May through the summer [*Goldammer et al.*, 2004; *Wotawa et al.*, 2006]. Both the fire pixel count and burned area are a factor of 3–4 larger than that in 2004 [*Wotawa et al.*, 2006]. In fact the burned area in 2003 was the largest in a decade. On the other hand, boreal forest fires in Alaska and Canada in summer were more intense in 2004 than in 2003. The burned area and fire counts were a factor of 2–3 larger in 2004 than in 2003. Although such boreal fires mainly influence the North America continent in the eastern and southeastern United States [*Wotawa and Trainer*, 2000], there is a discernable influence on the surrounding northeastern Pacific, as shown in the MODIS pollution aerosol map. In the midlatitude West Pacific, pollution largely from China influenced the region to the greatest extent in MAM and JJA, 2005. In the tropical East Pacific, the springtime biomass burning smoke from Central America was weakest in 2004.

[33] Table 2 compares annual pollution fluxes of east Asia outflow and North America inflow from 2002 to 2005. The annual pollution flux varies by as much as 25% for the

Table 2. Interannual Variations of Estimated Outflow and Inflow Pollution Fluxes

Year	East Asia Outflow, Tg/a	North America Inflow, Tg/a	Inflow/ Outflow, %
2002	15.8	3.7	23
2003	20.3	5.7	28
2004	16.0	4.2	26
2005	18.6	4.1	22
2002–2005	17.7	4.4	25

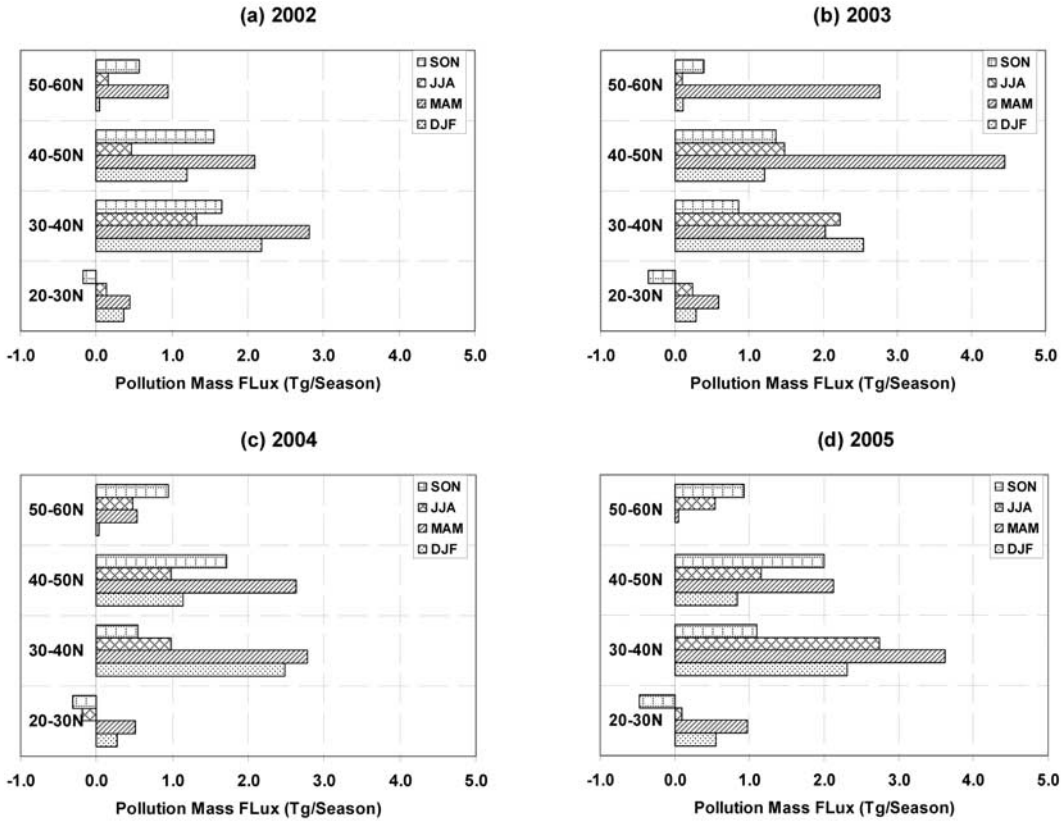

Figure 7. Interannual variations of east Asia outflow of pollution aerosol in different seasons and latitude segments derived from MODIS: (a) 2002, (b) 2003, (c) 2004, and (d) 2005.

outflow and 45% for the inflow. Both the outflow and inflow were strongest in 2003, because of record intense biomass burning emissions from spring to summer in Eurasia. About 20 Tg pollution aerosol was transported from east Asia to the northwestern Pacific, of which 28% reached the west coast of North America. This is followed by 2005 when 18.6 Tg pollution aerosol was exported from east Asia and 4.1 Tg was imported to North America. As discussed earlier, the pollution AOD in 2005 was higher than that in other years south of 40°N. While the pollution outflow was more or less of 16 Tg in 2002 and 2004, the inflow in 2002 is 12% smaller than that in 2004. The 4-year average pollution outflow is 17.7 Tg/a, of which about 25% (or 4.4 Tg/a) can reach the west coast of North America.

[34] The interannual variation of pollution fluxes depends strongly on season and latitude, as shown in Figure 7 for the east Asia outflow. In the 30–40°N segment, the springtime pollution flux in 2005 is about 180% higher than that in 2003, with that in 2002 and 2004 in between. The 2005 summertime pollution flux is a factor of 2–3 higher than that of 2002 and 2004, and 30% higher than that of 2003. In latitudes north of 40°N, the springtime pollution flux in 2003 is about a factor of 2 in 40–50°N and a factor of more than 3 higher in 50–60°N than that in other years, because of record intense boreal forest fires.

4.3. Estimated Uncertainties of Pollution Fluxes

[35] The above estimated pollution fluxes will inevitably be subject to uncertainties due to assumptions in implementing the algorithm. Major sources of uncertainties contributing to the pollution flux estimation integrated over latitudes and on annual average are listed in Table 3 and discussed as follows.

[36] One of first uncertainties would result from the MODIS-based estimate of anthropogenic aerosol optical depth. *Kaufman et al.* [2005b] estimated that the uncertainty in the derived anthropogenic AOD is 30%. Here we assume an uncertainty of 50% (corresponding to uncertainty factor of 1.5) to reflect potentially larger uncertainty on regional scales. In this study seasonal and geographical variations of maritime fine-mode fraction have been accounted for. However, a robust validation or evaluation is not possible

Table 3. Estimated Uncertainties in the Flux Calculation Resulting From Major Assumptions in Implementing the Algorithm[a]

Major Sources of Uncertainties	Estimated Uncertainty	Uncertainty Factor (UF)
Derivation of pollution AOD	50%	1.5
Aerosol mass extinction efficiency (dry) MEE	30%	1.3
Humidification factor for the extinction f(RH)	20%	1.2
Using monthly average polar-orbiting measurements (sampling and averaging)	15%	1.15
Transport heights	50%	1.5

[a]The overall uncertainty is estimated by assuming that the probability distribution function for each factor is log normal and individual sources of uncertainty are independent. Total uncertainty factor = $e^{(\sum_i (\log UF_i)^2)^{1/2}} = 1.96$.

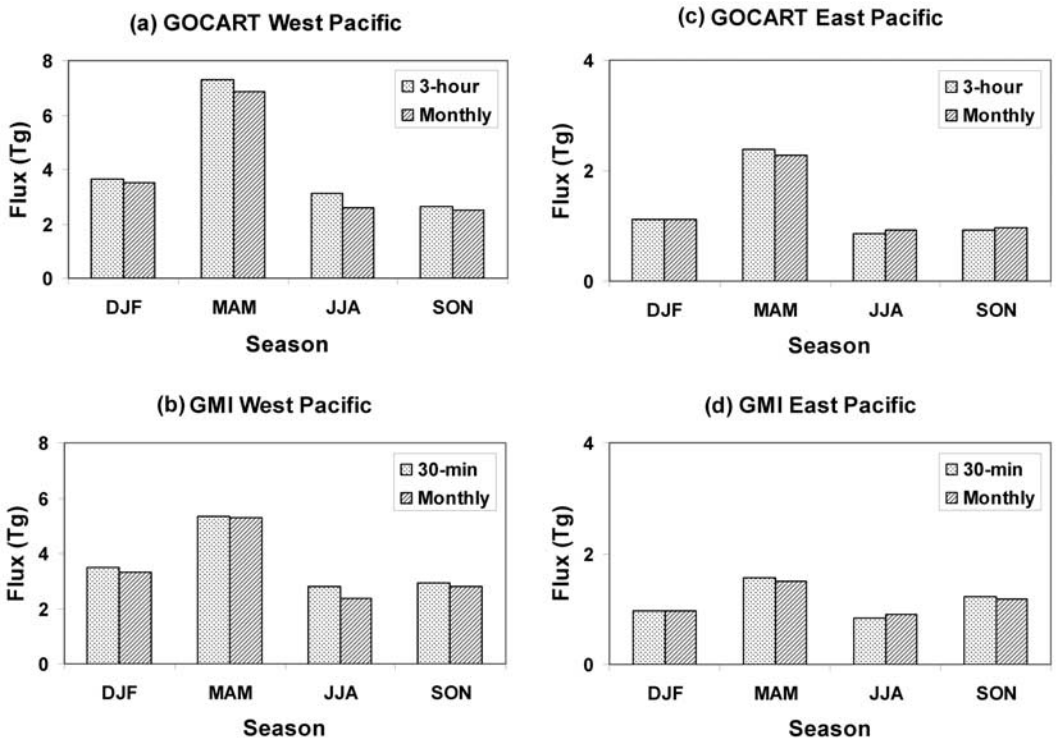

Figure 8. Comparisons of seasonal pollution fluxes over (a and b) West Pacific and (c and d) East Pacific diagnosed from model simulations at a frequency of 3 h for GOCART or 30 min for GMI with those calculated with monthly average aerosol and wind.

because of lack of observations of anthropogenic aerosol optical depth.

[37] The mass scattering efficiencies determined by aircraft and ship measurements are generally consistent [*Clarke et al.*, 2002] and their uncertainty comes from measurements of aerosol mass and scattering, which is estimated to be about 25% [*Quinn et al.*, 2004]. The uncertainty for the single-scattering albedo is estimated to be 10%. These result in an estimate of overall uncertainty for the mass extinction efficiency to be 30%. For the fractional change in aerosol scattering as a function of RH, measurements from two nephelometers agreed within 10% [*Carrico et al.*, 2003]. For pollution aerosol, the hysteresis factor, a ratio of scattering coefficient on the monotonic to deliquescent curves of the hysteresis loop, is estimated to be 1.3 at RH = 60% [*Carrico et al.*, 2003]. The use of average of monotonic and deliquescent growth curve would introduce an error of 15%. Therefore we estimate an overall uncertainty of 20% for f(RH).

[38] Polar-orbiting satellite sensors can only observe aerosols once daily and a combined use of the same MODIS sensor onboard the twin EOS satellites Terra (10:30AM local time) and Aqua (1:30PM local time) allows twice daily observations of aerosols in a region. While MODIS Terra and Aqua measurements on average well represent the daily aerosol optical depth on a global scale [*Kaufman et al.*, 2000, 2005c] and in east Asia [*Smirnov et al.*, 2002], it is not clear if MODIS-based estimates of pollution fluxes are a good representation of the daily average. Our sensitivity tests suggest that the GOCART calculated fluxes around the Terra/Aqua overpass times generally differ from the GOCART day and night averages by about 10% in the region. A use of monthly averaged MODIS aerosol and wind speed for calculating pollution fluxes may introduce additional uncertainties if the pollution aerosol mass loading correlates highly with the east-west component of wind speed. Here we use GOCART and GMI model simulations to examine differences between fluxes diagnosed from 30-min (for GMI) and 3-h (for GOCART) simulations of aerosol and wind and those using corresponding monthly average aerosol and wind. As shown in Figure 8, the differences in pollution fluxes are generally less than 6%, with an exception for the summertime east Asia outflow where the differences are about 15%. Here we assign an overall uncertainty of 15% for the above sampling and averaging processes in our MODIS-based estimates.

[39] The determination of transport heights of pollution aerosol plume has been used for dual purposes, i.e., selecting representative RH to account for humidification growth of aerosol and selecting representative wind speed for calculating mass fluxes. In this study, we have partitioned pollution AOD into 3 vertical segments of 0–1, 1–2, and above 2 km with equal fractions; a higher transport height (i.e., a larger fraction at higher altitudes) would result in larger aerosol mass flux because of stronger wind speed and drier air mass (hence greater aerosol mass for a given optical depth) at high altitudes in general. The sensitivity of pollution mass flux to the transport height should vary with region, depending on patterns of wind shear and atmospheric humidity. To examine such sensitivity, we assume pollution aerosol is evenly distributed in four vertical layers up to

an altitude of 5 km and wind and humidity at 925, 850, 700, and 600 hPa are used to calculate aerosol mass loading and fluxes in individual layers respectively. In comparison to the original assumption of vertical distribution, the pollution flux increases by 20–80%, depending on season and latitude. By integrating over all latitudes, the east Asia outflow and North America inflow increases by 40–60% and 30–40%, respectively. An average uncertainty of 50% is assigned for the assumption of transport heights.

[40] We assumed that the probability distribution function for each factor was log normal and individual uncertainties were independent, the overall uncertainty factor in the calculated annual pollution aerosol fluxes was estimated as about 2. This gives a range of 9–35 Tg/a and 2–9 Tg/a for the estimated outflow and inflow of pollution aerosol flux, respectively. The estimated uncertainty presumably represents a lower bound because the sources of error were assumed to be independent. The uncertainties would also be larger in some subregions and seasons. While biomass burning smoke can come from both natural and man made fires, it remains challenging to make an unambiguous distinction between them. Our assumption that all biomass burning aerosols are pollution would have biased our estimates of pollution fluxes in high latitudes in spring and summer where Eurasia boreal forest fires usually occur. On the other hand, the determination of transport heights and hygroscopic properties of pollution aerosol in this study is largely based on field experiments that have focused on industrial/urban pollution. This may have underestimated the flux of smoke aerosol because smoke aerosol can be raised to higher altitudes where wind speed is generally stronger, humidity is lower, and smoke aerosol usually has lower hygroscopicity (i.e., a larger mass loading for smoke than for industrial pollution for a given AOD).

[41] In this study we use the monthly mean dry aerosol mass derived from satellite retrievals in cloud-free conditions to calculate transport flux of pollution aerosol. Inherent in these estimates of pollutant transport is the assumption that the dry mass transport over the course of a month is the same, whether or not there are frontal cloud systems in the region. Frontal cloud systems extend over wide areas, preventing aerosol retrievals in those areas. These are not the same as broken cloud fields where satellite retrievals of aerosols are possible in the holes between clouds. For example, because aerosol transport is associated with the WCB, and the WCB is associated with rising air in warm fronts that also consist of wide spread cloudiness, MODIS may miss important transport events every month. If dry aerosol mass in these events is significantly different from the monthly mean observed in cloud-free conditions, the estimated pollutant flux may have large uncertainties or biases. It has been suggested that a variety of compensating processes in and nearby clouds control the formation and removal of aerosols and hence determine their loading. While clouds can effectively remove aerosols from atmosphere through scavenging and rainout, they can also generate aerosol (e.g., in-cloud aqueous production of sulfate). We do not know how to quantify the differences in dry aerosol mass between cloud-free conditions and frontal cloud systems, and whether an overall bias exists in the estimated pollution fluxes. However, we acknowledge that the factor of 2 uncertainty calculated from the known and presumably independent uncertainties may be a conservative number.

[42] A reduction of uncertainty in the estimated pollution aerosol fluxes can be achieved through integrating measurements from other A-Train sensors flying in formation with MODIS. For example, the new capabilities of passive remote sensing such as MODIS should be further enhanced by emerging lidar measurements of aerosol vertical distributions made by CALIPSO [*Winker et al.*, 2003]. GLAS data with limited temporal coverage has been used in this study to help determine aerosol transport heights. However, the availability of only 532 nm GLAS data makes it difficult to separate pollution aerosol from dust. Since June 2006, CALIPSO has been sensing the vertical distributions of aerosol backscatter and extinction in continuous mode, enhancing the temporal coverage of data. Furthermore the use of the two wavelengths and the depolarization capability at 532 nm of CALIOP can be used to better categorize aerosol types. In the future, fully calibrated and validated CALIPSO aerosol extinction/backscatter profile data can be used to achieve a better quantification of aerosol intercontinental transport, in terms of seasonal, interannual, and geographical variations. A retrieval of fine and coarse-mode separated aerosol extinction profile with a fusion of CALIOP and MODIS/POLDER measurements [*Kaufman et al.*, 2003a, 2003b] would make a reliable estimate of vertical distributions of aerosol mass flux possible.

[43] The Polarization and Directionality of the Earth's Reflectance (POLDER) on the Polarization and Anisotropy of Reflectance for Atmospheric Science coupled with Observations from a Lidar (PARASOL) is measuring directional and polarized radiance in nine spectral channels from 443 nm to 1020 nm. In addition to retrievals of AOD and size parameters, the analysis of the polarized angular scattered radiance provides additional information on the shape of particles (e.g., spherical versus nonspherical) [*Herman et al.*, 2005]. This complements the MODIS spectral measurements which are not sensitive to particle shape and can be used to separate nonspherical dust from spherical maritime aerosols [*Gérárd et al.*, 2005]. The Ozone Monitoring Instrument (OMI) onboard Aura since 2005 can separate UV-absorbing mineral dust or biomass burning smoke from scattering sulfate aerosol [*Herman et al.*, 1997]. Such information could help determine if the plume is dominated by industrial pollution or smoke and hence make a better characterization of aerosol growth with relative humidity.

5. Summary and Conclusion

[44] By taking advantage of MODIS high-accuracy measurements of aerosol optical depth and fine-mode fraction over oceans, we have developed an observation-based approach to estimate the intercontinental transport of pollution aerosol over the North Pacific. For this method, measurements from other satellite sensors, such as AIRS and GLAS, and from field campaigns have also been used. We estimated that for 2002–2005 average, about 18 Tg/a of pollution aerosol is exported from Asia, of which about 25% arrives in the west coast of North America. The imported flux of 4.4 Tg/a to North America is equivalent to about 15% of local emissions from the United States and

Canada as reported in literature [e.g., *Chin et al.*, 2007]. The export and import pollution fluxes are largest in spring and smallest in summer, with the springtime and summertime flux accounting for about 40% and 10% of the annual integrated flux, respectively. For the period we have examined, the strongest pollution export occurred in 2003, due largely to record intense boreal forest fires in Eurasia. The overall uncertainty for pollution fluxes is estimated at a factor of about 2, resulting from separating pollution aerosol from dust and maritime aerosol, deriving the aerosol mass loading and determining the transport heights of the pollution plume. A reduction of uncertainty can be achieved with a better characterization of pollution aerosol through integrating the PARASOL measurements of spherical and nonspherical aerosols, CALIPSO measurements of vertical distributions of pollution aerosol, and OMI aerosol indices. Simulations by GOCART and GMI models agree quite well with the satellite-based estimates of annual and latitude-integrated fluxes, with larger model-satellite differences in latitudinal variations of fluxes. The satellite-based approach developed in this study can be adapted and extended to study the intercontinental transport of pollution in other regions.

[45] While this study shows that a substantial amount of pollution aerosol from Asia can be transported to North America, its implications for climate change and air quality have not been assessed. Both modeling studies with reliable representations of major transport mechanisms at a wide range of scales and analyses of CALIPSO aerosol vertical distributions are necessary for gaining insights of downward transport of the height-elevated pollution to the atmospheric boundary layer and of potential influences of Asian pollution aerosol on surface air quality in North America. Further research is needed to assess how the intercontinental transport of pollution aerosol can influence the weather and climate over the North Pacific and how the resulting changes in atmospheric circulations would feedback on the transpacific transport of pollution and dust. Long-term trends in the transpacific pollution transport and its environmental impacts would be detected with an accumulation of satellite data in the future.

[46] **Acknowledgments.** We dedicate this paper to our mentor and colleague, Yoram J. Kaufman, who died in an accident in May 2006, for his inspiration and encouragement. We are grateful to two reviewers for helpful comments and suggestions. Our thanks also go to Steve Palm and Tom Kucsera for helping on the use of GLAS data. H.Y. was supported by the NASA Atmospheric Composition Modeling and Analysis program (ACMAP).

References

Akimoto, H., T. Ohara, J. Kurokawa, and N. Horii (2006), Verification of energy consumption in China during 1996–2003 by using satellite observational data, *Atmos. Environ.*, *40*, 7663–7667, doi:10.1016/j.atmosenv.2006.07.052.

Al-Saadi, J., et al. (2005), Improving national air quality forecasts with satellite aerosol observations, *Bull. Am. Meteorol. Soc.*, *86*(9), 1249–1261, doi:10.1175/BAMS-86-9-1249.

Anderson, T. L., et al. (2005), A-Train strategy for quantifying direct climate forcing by aerosols, *Bull. Am. Meteorol. Soc.*, *86*(12), 1795–1809, doi:10.1175/BAMS-86-12-1795.

Andreae, M. O., et al. (1988), Vertical distribution of dimethylsulfide, sulfur dioxide, aerosol ions, and radon over the northeast Pacific Ocean, *J. Atmos. Chem.*, *6*, 149–173, doi:10.1007/BF00048337.

Aumann, H., et al. (2003), AIRS/AMSU/HSB on the Aqua mission: Design, science objectives, data products, and processing system, *IEEE Trans. Geosci. Remote Sens.*, *41*(2), 253–264, doi:10.1109/TGRS.2002.808356.

Bahreini, R., et al. (2003), Aircraft-based aerosol size and composition measurements during ACE-Asia using an Aerodyne aerosol mass spectrometer, *J. Geophys. Res.*, *108*(D23), 8645, doi:10.1029/2002JD003226.

Bates, T. S., et al. (2001), Regional physical and chemical properties of the marine boundary layer aerosol across the Atlantic during Aerosols99: An overview, *J. Geophys. Res.*, *106*(D18), 20,767–20,782, doi:10.1029/2000JD900578.

Bates, T. S., et al. (2006), Aerosol direct radiative effects over the northwest Atlantic, northwest Pacific, and North Indian Oceans: Estimates based on in-situ chemical and optical measurements and chemical transport modeling, *Atmos. Chem. Phys.*, *6*, 1657–1732.

Bellouin, N., O. Boucher, J. Haywood, and M. S. Reddy (2005), Global estimate of aerosol direct radiative forcing from satellite measurements, *Nature*, *438*(7071), 1138–1141, doi:10.1038/nature04348.

Bertschi, I. T., D. A. Jaffe, L. Jaegle, H. U. Price, and J. B. Dennison (2004), PHOBEA/ITCT200 2 airborne observations of transpacific transport of ozone, CO, volatile organic compounds, and aerosols to the northeast Pacific: Impacts of Asian anthropogenic and Siberian boreal fire emissions, *J. Geophys. Res.*, *109*, D23S12, doi:10.1029/2003JD004328.

Bian, H., M. Chin, R. Kawa, B. Duncan, A. Arellano Jr., and R. Kasibhatla (2007), Sensitivity of global CO simulations to uncertainties in biomass burning sources, *J. Geophys. Res.*, *112*, D23308, doi:10.1029/2006JD008376.

Biscaye, P. E., F. E. Grousset, A. M. Svensson, and A. Bory (2000), Eurasian air pollution reaches eastern North America, *Science*, *290*, 2258–2259, doi:10.1126/science.290.5500.2258.

Bond, T., D. Streets, K. Yarber, S. Nelson, J. Woo, and Z. Klimont (2004), A technology-based inventory of black and organic carbon emissions from combustion, *J. Geophys. Res.*, *109*, D14203, doi:10.1029/2003JD003697.

Carmichael, G., D. Streets, G. Calori, M. Amann, M. Z. Jacobson, J. Hansen, and H. Ueda (2002), Changing trends in sulfur emissions in Asia: Implications for acid deposition, air pollution, and climate, *Environ. Sci. Technol.*, *36*, 4707–4713.

Carrico, C. M., P. Kus, M. J. Rood, P. K. Quinn, and T. S. Bates (2003), Mixtures of pollution, dust, sea salt, and volcanic aerosol during ACE-Asia: Radiative properties as a function of relative humidity, *J. Geophys. Res.*, *108*(D23), 8650, doi:10.1029/2003JD003405.

Chameides, W. L., et al. (1999), A case study of the effects of atmospheric aerosols and regional haze on agriculture: An opportunity to enhance crop yields in China through emission controls?, *Proc. Natl. Acad. Sci. U. S. A.*, *96*(24), 13,626–13,633, doi:10.1073/pnas.96.24.13626.

Chin, M., R. B. Rood, S.-J. Lin, J. F. Muller, and A. M. Thompson (2000a), Atmospheric sulfur cycle in the global model GOCART: Model description and global properties, *J. Geophys. Res.*, *105*, 24,671–24,687, doi:10.1029/2000JD900384.

Chin, M., et al. (2000b), Atmospheric sulfur cycle in the global model GOCART: Comparison with field observations and regional budgets, *J. Geophys. Res.*, *105*, 24,689–24,712, doi:10.1029/2000JD900385.

Chin, M., et al. (2002), Tropospheric aerosol optical thickness from the GOCART model and comparisons with satellite and sunphotometer measurements, *J. Atmos. Sci.*, *59*, 461–483, doi:10.1175/1520-0469(2002)059<0461:TAOTFT>2.0.CO;2.

Chin, M., P. Ginoux, R. Lucchesi, B. Huebert, R. Weber, T. Anderson, S. Masonis, B. Blomquist, A. Bandy, and D. Thornton (2003), A global aerosol model forecast for the ACE-Asia field experiment, *J. Geophys. Res.*, *108*(D23), 8654, doi:10.1029/2003JD003642.

Chin, M., et al. (2004), Aerosol distribution in the Northern Hemisphere during ACE-Asia: Results from global model, satellite observations, and Sun photometer measurements, *J. Geophys. Res.*, *109*, D23S90, doi:10.1029/2004JD004829.

Chin, M., T. Diehl, P. Ginoux, and W. Malm (2007), Intercontinental transport of pollution and dust aerosols: implications for regional air quality, *Atmos. Chem. Phys.*, *7*, 5501–5517.

Christopher, S. A., et al. (2006), Satellite-based assessment of top of atmosphere anthropogenic aerosol radiative forcing over cloud-free oceans, *Geophys. Res. Lett.*, *33*, L15816, doi:10.1029/2005GL025535.

Chung, Y. S. (1986), Air pollution detection by satellites: The transport and deposition of air pollutants over oceans, *Atmos. Environ.*, *20*, 617–630, doi:10.1016/0004-6981(86)90177-0.

Clarke, A. D., et al. (2002), INDOEX aerosol: A comparison and summary of chemical, microphysical, and optical properties observed from land, ship, and aircraft, *J. Geophys. Res.*, *107*(D19), 8033, doi:10.1029/2001JD000572.

de Gouw, J. A., et al. (2004), Chemical composition of air masses transported from Asia to the U.S. West Coast during ITCT 2K2: Fossil fuel combustion versus biomass-burning signatures, *J. Geophys. Res.*, *109*, D23S20, doi:10.1029/2003JD004202.

Dibb, J. E., et al. (2003), Aerosol chemical composition in Asian continental outflow during the TRACE-P campaign: Comparison with PEM-West B, *J. Geophys. Res.*, *108*(D21), 8815, doi:10.1029/2002JD003111.

Dickerson, R. R., et al. (2007), Aircraft observations of dust and pollutants over NE China: Insight into the meteorological mechanisms of long-range transport, *J. Geophys. Res.*, *112*, D24S90, doi:10.1029/2007JD008999.

Duce, R. A., C. K. Unni, and B. J. Ray (1980), Long-range atmospheric transport of soil dust from Asia to the tropical North Pacific: Temporal variability, *Science*, *209*(4464), 1522–1524, doi:10.1126/science.209.4464.1522.

Duncan, B. N., R. V. Martin, A. C. Staudt, R. Yevich, and J. A. Logan (2003), Interannual and seasonal variability of biomass burning emissions constrained by satellite observations, *J. Geophys. Res.*, *108*(D2), 4100, doi:10.1029/2002JD002378.

Eckhardt, S., et al. (2004), A 15-year climatology of warm conveyor belts, *J. Clim.*, *17*, 218–237, doi:10.1175/1520-0442(2004)017<0218:AYCOWC>2.0.CO;2.

Engel-Cox, J. A., C. H. Hollloman, B. W. Coutant, and R. M. Hoff (2004), Qualitative and quantitative evaluation of MODIS satellite sensor data for regional and urban scale air quality, *Atmos. Environ.*, *38*, 2495–2509, doi:10.1016/j.atmosenv.2004.01.039.

Fairlie, T. D., D. J. Jacob, and R. J. Park (2007), The impact of transpacific transport of mineral dust in the United States, *Atmos. Environ.*, *41*, 1251–1266, doi:10.1016/j.atmosenv.2006.09.048.

Fraser, R. S. (1976), Satellite measurement of mass of Sahara dust in the atmosphere, *Appl. Opt.*, *15*, 2471–2479.

Fraser, R. S., Y. J. Kaufman, and R. L. Mahoney (1984), Satellite measurements of aerosol mass and transport, *Atmos. Environ.*, *18*, 2577–2584, doi:10.1016/0004-6981(84)90322-6.

Gérárd, B., et al. (2005), Comparisons between POLDER2 and MODIS/Terra aerosol retrievals over ocean, *J. Geophys. Res.*, *110*, D24211, doi:10.1029/2005JD006218.

Giglio, L., G. R. van der Werf, J. T. Randerson, G. J. Collatz, and P. Kasibhatla (2006), Global estimation of burned area using MODIS active fire observations, *Atmos. Chem. Phys.*, *6*, 957–974.

Ginoux, P., M. Chin, I. Tegen, J. Prospero, B. Holben, O. Dubovik, and S.-J. Lin (2001), Sources and distributions of dust aerosols simulated with the GOCART model, *J. Geophys. Res.*, *106*, 20,255–20,273, doi:10.1029/2000JD000053.

Ginoux, P., J. Prospero, O. Torres, and M. Chin (2004), Long-term simulation of dust distribution with the GOCART model: Correlation with the North Atlantic Oscillation, *Environ. Model. Softw.*, *19*, 113–128, doi:10.1016/S1364-8152(03)00114-2.

Goldammer, J. G., A. Sukhinin, and I. Csiszar (2004), The current fire situation in the Russian Federation: Implications for enhancing international and regional cooperation in the UN framework and the global programs on fire monitoring and assessment, *Int. For. Fire News*, *29*, 89–111.

Grousset, F., P. Ginoux, A. Bory, and P. E. Biscaye (2003), Case study of a Chinese dust plume reaching the French Alps, *Geophys. Res. Lett.*, *30*(6), 1277, doi:10.1029/2002GL016833.

Hadley, O. L., V. Ramanathan, G. R. Carmichael, Y. Tang, C. E. Corrigan, G. C. Roberts, and G. S. Mauger (2007), Trans-Pacific transport of black carbon and fine aerosols (D < 2.5 μm) into North America, *J. Geophys. Res.*, *112*, D05309, doi:10.1029/2006JD007632.

Hansen, J., and L. Nazarenko (2004), Soot climate forcing via snow and ice albedos, *Proc. Natl. Acad. Sci. U. S. A.*, *101*(2), 423–428, doi:10.1073/pnas.2237157100.

Heald, C. L., et al. (2003), Asian outflow and trans-Pacific transport of carbon monoxide and ozone pollution: An integrated satellite, aircraft, and model perspective, *J. Geophys. Res.*, *108*(D24), 4804, doi:10.1029/2003JD003507.

Heald, C. L., et al. (2006), Transpacific transport of Asian anthropogenic aerosols and its impact on surface air quality in the United States, *J. Geophys. Res.*, *111*, D14310, doi:10.1029/2005JD006847.

Herman, J., P. Bhartia, O. Torres, C. Hsu, C. Seftor, and E. Celarier (1997), Global distribution of UV-absorbing aerosols from Nimbus-7/TOMS data, *J. Geophys. Res.*, *102*, 16,911–16,922, doi:10.1029/96JD03680.

Herman, M., J. L. Deuzé, A. Marchand, B. Roger, and P. Lallart (2005), Aerosol remote sensing from POLDER/ADEOS over the ocean: Improved retrieval using a nonspherical particle model, *J. Geophys. Res.*, *110*, D10S02, doi:10.1029/2004JD004798.

Higurashi, A., and T. Nakajima (2002), Detection of aerosol types over the East China Sea near Japan from four-channel satellite data, *Geophys. Res. Lett.*, *29*(17), 1836, doi:10.1029/2002GL015357.

Holzer, M., T. M. Hall, and R. B. Stull (2005), Seasonality and weather-driven variability of transpacific transport, *J. Geophys. Res.*, *110*, D23103, doi:10.1029/2005JD006261.

Huang, Y., R. E. Dickinson, and W. L. Chameides (2006), Impact of aerosol indirect effect on surface temperature over east Asia, *Proc. Natl. Acad. Sci. U. S. A.*, *103*(12), 4371–4376, doi:10.1073/pnas.0504428103.

Huebert, B. J., et al. (2003), An overview of ACE-Asia: Strategies for quantifying the relationships between Asian aerosols and their climatic impacts, *J. Geophys. Res.*, *108*(D23), 8633, doi:10.1029/2003JD003550.

Huebert, B. J., T. Bertram, J. Kline, S. Howell, D. Eatough, and B. Blomquist (2004), Measurements of organic and elemental carbon in Asian outflow during ACE-Asia from the NSF/NCAR C-130, *J. Geophys. Res.*, *109*, D19S11, doi:10.1029/2004JD004700.

Husar, R. B., et al. (2001), The Asian dust events of April, 1998, *J. Geophys. Res.*, *106*, 18,317–18,330, doi:10.1029/2000JD900788.

Jacob, D. J., et al. (2003), The transport and chemical evolution over the Pacific (TRACE-P) aircraft mission: Design, execution, and first results, *J. Geophys. Res.*, *108*(D20), 9000, doi:10.1029/2002JD003276.

Jaffe, D., et al. (1999), Transport of Asian air pollution to North America, *Geophys. Res. Lett.*, *26*, 711–714, doi:10.1029/1999GL900100.

Jaffe, D., S. Tamura, and J. Harris (2005), Seasonal cycle and composition of background fine particles along the west coast of the US, *Atmos. Environ.*, *39*, 297–306, doi:10.1016/j.atmosenv.2004.09.016.

Jirak, I. L., and W. R. Cotton (2006), Effect of air pollution on precipitation along the Front Range of the Rocky Mountains, *J. Appl. Meteorol. Climatol.*, *45*, 236–245, doi:10.1175/JAM2328.1.

Kaufman, Y. J., D. Tanré, L. Remer, E. Vermote, A. Chu, and B. N. Holben (1997), Operational remote sensing of tropospheric aerosol over land from EOS Moderate Resolution Imaging Spectroradiometer, *J. Geophys. Res.*, *102*, 17,051–17,067, doi:10.1029/96JD03988.

Kaufman, Y. J., B. N. Holben, D. Tanré, I. Slutsker, A. Smirnov, and T. F. Eck (2000), Will aerosol measurements from Terra and Aqua polar orbiting satellites represent daily aerosol abundance and properties?, *Geophys. Res. Lett.*, *27*, 3861–3864, doi:10.1029/2000GL011968.

Kaufman, Y. J., D. Tanré, and O. Boucher (2002), A satellite view of aerosols in the climate system, Review, *Nature*, *419*, 215–223, doi:10.1038/nature01091.

Kaufman, Y. J., J. M. Haywood, P. V. Hobbs, W. Hart, R. Kleidman, and B. Schmid (2003a), Remote sensing of vertical distributions of smoke aerosol off the coast of Africa, *Geophys. Res. Lett.*, *30*(16), 1831, doi:10.1029/2003GL017068.

Kaufman, Y. J., D. Tanré, J.-F. León, and J. Pelon (2003b), Retrievals of profiles of fine and coarse aerosols using lidar and radiometric space measurements, *IEEE Trans. Geosci. Remote Sens.*, *41*(8), 1743–1754, doi:10.1109/TGRS.2003.814138.

Kaufman, Y. J., I. Koren, L. A. Remer, D. Tanré, P. Ginoux, and S. Fan (2005a), Dust transport and deposition observed from the Terra-Moderate Resolution Imaging Spectroradiometer (MODIS) spacecraft over the Atlantic Ocean, *J. Geophys. Res.*, *110*, D10S12, doi:10.1029/2003JD004436.

Kaufman, Y. J., O. Boucher, D. Tanré, M. Chin, L. A. Remer, and T. Takemura (2005b), Aerosol anthropogenic component estimated from satellite data, *Geophys. Res. Lett.*, *32*, L17804, doi:10.1029/2005GL023125.

Kaufman, Y. J., et al. (2005c), A critical examination of the residual cloud contamination and diurnal sampling effects on MODIS estimates of aerosol over ocean, *IEEE Trans. Geosci. Remote Sens.*, *43*(12), 2886–2897.

Kaufman, Y. J., I. Koren, L. A. Remer, D. Rosenfeld, and Y. Rudich (2005d), The effect of smoke, dust and pollution aerosol on shallow cloud development over the Atlantic Ocean, *Proc. Natl. Acad. Sci. U. S. A.*, *102*(32), 11,207–11,212, doi:10.1073/pnas.0505191102.

Kim, S., S. Yoon, J. Kim, and S. Kim (2007), Seasonal and monthly variations of columnar aerosol optical properties over east Asia determined from multi-year MODIS, LIDAR, and AERONET Sun/sky radiometer measurements, *Atmos. Environ.*, *41*, 1634–1651, doi:10.1016/j.atmosenv.2006.10.044.

King, M. D., Y. J. Kaufman, D. Tanré, and T. Nakajima (1999), Remote sensing of tropospheric aerosols: Past, present, and future, *Bull. Am. Meteorol. Soc.*, *80*, 2229–2259, doi:10.1175/1520-0477(1999)080<2229:RSOTAF>2.0.CO;2.

Kleidman, R. G., et al. (2005), Comparison of Moderate Resolution Imaging Spectroradiometer (MODIS) and Aerosol Robotic Network (AERONET) remote-sensing retrievals of aerosol fine mode fraction over ocean, *J. Geophys. Res.*, *110*, D22205, doi:10.1029/2005JD005760.

Koren, I., Y. J. Kaufman, L. A. Remer, and V. Martin (2004), Measurement of the effect of Amazon smoke on inhibition of cloud formation, *Science*, *303*, 1342–1345, doi:10.1126/science.1089424.

León, J.-F., D. Tanré, J. Pelon, Y. J. Kaufman, J. M. Haywood, and B. Chatenet (2003), Profiling of a Saharan dust outbreak based on a synergy between active and passive remote sensing, *J. Geophys. Res.*, *108*(D18), 8575, doi:10.1029/2002JD002774.

Levy, R., L. A. Remer, S. Mattoo, E. Vermote, and Y. Kaufman (2007), Second-generation algorithm for retrieving aerosol properties over land from MODIS spectral reflectance, *J. Geophys. Res.*, *112*, D13211, doi:10.1029/2006JD007811.

Liang, Q., L. Jaegle, D. A. Jaffe, P. Weiss-Penzias, A. Heckman, and J. A. Snow (2004), Long-range transport of Asian pollution to the northeast Pacific: Seasonal variations and transport pathways of carbon monoxide, *J. Geophys. Res.*, *109*, D23S07, doi:10.1029/2003JD004402.

Liu, H., D. J. Jacob, I. Bey, R. M. Yantosca, B. N. Duncan, and G. W. Sachse (2003), Transport pathways for Asian pollution outflow over the Pacific: Interannual and seasonal variations, *J. Geophys. Res.*, *108*(D20), 8786, doi:10.1029/2002JD003102.

Liu, J., D. L. Mauzerall, and L. W. Horowitz (2005), Analysis of seasonal and interannual variability in transpacific transport, *J. Geophys. Res.*, *110*, D04302, doi:10.1029/2004JD005207.

Liu, X., J. Penner, B. Das, D. Bergmann, J. Rodriguez, S. Strahan, M. Wang, and Y. Feng (2007), Uncertainties in global aerosol simulations: Assessment using three meteorological data sets, *J. Geophys. Res.*, *112*, D11212, doi:10.1029/2006JD008216.

Lyons, W. A., J. C. Dooley Jr., and K. T. Whitby (1978), Satellite detection of long-range pollution transport and sulfate aerosol hazes, *Atmos. Environ.*, *12*, 621–631, doi:10.1016/0004-6981(78)90242-1.

McKendry, I. G., et al. (2001), Long-range transport of Asian dust to the Lower Fraser Valley, British Columbia, Canada, *J. Geophys. Res.*, *106*(D16), 18,361–18,370, doi:10.1029/2000JD900359.

Menon, S., J. E. Hansen, L. Nazarenko, and Y. Luo (2002), Climate effects of black carbon aerosols in China and India, *Science*, *297*, 2250–2253, doi:10.1126/science.1075159.

Newell, R. E., and M. J. Evans (2000), Seasonal changes in pollutant transport to the North Pacific: the relative importance of Asian and European sources, *Geophys. Res. Lett.*, *27*, 2509–2512, doi:10.1029/2000GL011501.

Parrish, D. D., et al. (2004), Intercontinental Transport and Chemical Transformation 2002 (ITCT 2K2) and Pacific Exploration of Asian Continental Emission (PEACE) experiments: An overview of the 2002 winter and spring intensives, *J. Geophys. Res.*, *109*, D23S01, doi:10.1029/2004JD004980.

Price, H. U., D. A. Jaffe, P. V. Doskey, I. McKendry, and T. L. Anderson (2003), Vertical profiles of O3, aerosol, CO, NMHCs in the Northeast Pacific during the TRACE-P and ACE-Asia experiments, *J. Geophys. Res.*, *108*(D20), 8799, doi:10.1029/2002JD002930.

Qian, Y., W. Wang, L. Leung, and D. Kaiser (2007), Variability of solar radiation under cloud-free skies in China: The role of aerosols, *Geophys. Res. Lett.*, *34*, L12804, doi:10.1029/2006GL028800.

Quinn, P. K., et al. (2004), Aerosol optical properties measured on board the Ronald H. Brown during ACE-Asia as a function of aerosol chemical composition and source region, *J. Geophys. Res.*, *109*, D19S01, doi:10.1029/2003JD004010.

Quinn, P. K., et al. (2005), Impact of particulate organic matter on the relative humidity dependence of light scattering: A simplified parameterization, *Geophys. Res. Lett.*, *32*, L22809, doi:10.1029/2005GL024322.

Remer, L. A., and Y. J. Kaufman (2006), Aerosol direct radiative effect at the top of the atmosphere over cloud free ocean derived from four years of MODIS data, *Atmos. Chem. Phys.*, *6*, 237–253.

Remer, L. A., et al. (2002), Validation of MODIS aerosol retrieval over ocean, *Geophys. Res. Lett.*, *29*(12), 8008, doi:10.1029/2001GL013204.

Remer, L. A., et al. (2005), The MODIS aerosol algorithm, products, and validation, *J. Atmos. Sci.*, *62*, 947–973, doi:10.1175/JAS3385.1.

Richter, A., P. Burrows, H. Nues, C. Granier, and U. Niemeijer (2005), Increase in tropospheric nitrogen dioxide over China observed from space, *Nature*, *437*, 129–130, doi:10.1038/nature04092.

Rosenfeld, D., and A. Givati (2006), Evidence of orographic precipitation suppression by air pollution-induced aerosols in the western United States, *J. Appl. Meteorol. Climatol.*, *45*, 893–911, doi:10.1175/JAM2380.1.

Sassen, K. (2002), Indirect climate forcing over the western US from Asian dust storms, *Geophys. Res. Lett.*, *29*(10), 1465, doi:10.1029/2001GL014051.

Shinozuka, Y., et al. (2004), Sea-salt vertical profiles over the southern and tropical Pacific oceans: Microphysics, optical properties, spatial variability, and variations with wind speed, *J. Geophys. Res.*, *109*, D24201, doi:10.1029/2004JD004975.

Smirnov, A., B. N. Holben, T. F. Eck, I. Slutsker, B. Chatenet, and R. T. Pinker (2002), Diurnal variability of aerosol optical depth observed at AERONET (Aerosol Robotic Network) sites, *Geophys. Res. Lett.*, *29*(23), 2115, doi:10.1029/2002GL016305.

Spinhirne, J. D., S. P. Palm, W. D. Hart, D. L. Hlavka, and E. J. Welton (2005), Cloud and aerosol measurements from the GLAS space borne lidar: Initial results, *Geophys. Res. Lett.*, *32*, L22S03, doi:10.1029/2005GL023507.

Stohl, A. (2001), A one-year Lagrangian "climatology" of airstreams in the northern hemisphere troposphere and lowermost stratosphere, *J. Geophys. Res.*, *106*, 7263–7279, doi:10.1029/2000JD900570.

Stohl, A., S. Eckhardt, C. Forster, P. James, and N. Spichtinger (2002), On the pathways and timescales of intercontinental air pollution transport, *J. Geophys. Res.*, *107*(D23), 4684, doi:10.1029/2001JD001396.

Stohl, A., et al. (2007), Aircraft measurements over Europe of an air pollution plume from Southeast Asia—Aerosol and chemical characterization, *Atmos. Chem. Phys.*, *7*, 913–937.

Tan, Q., Y. Huang, and W. L. Chameides (2002), Budget and export of anthropogenic SOx from east Asia during continental outflow conditions, *J. Geophys. Res.*, *107*(D13), 4167, doi:10.1029/2001JD000769.

Tanré, D., Y. J. Kaufman, M. Herman, and S. Mattoo (1997), Remote sensing of aerosol properties over oceans using the MODIS/EOS spectral radiances, *J. Geophys. Res.*, *102*, 16,971–16,988, doi:10.1029/96JD03437.

Tanré, D., F. M. Bréon, J. L. Deuzé, M. Herman, P. Goloub, F. Nadal, and A. Marchand (2001), Global observation of anthropogenic aerosols from satellite, *Geophys. Res. Lett.*, *28*(24), 4555–4558, doi:10.1029/2001GL013036.

VanCuren, R. A., and T. A. Cahill (2002), Asian aerosols in North America: Frequency and concentration of fine dust, *J. Geophys. Res.*, *107*(D24), 4804, doi:10.1029/2002JD002204.

VanCuren, R. A., S. S. Cliff, K. D. Perry, and M. Jimenez-Cruz (2005), Asian continental aerosol persistence above the marine boundary layer over the eastern North Pacific: Continuous aerosol measurements from International Transport and Chemical Transformation 2002 (ITCT 2K2), *J. Geophys. Res.*, *110*, D09S90, doi:10.1029/2004JD004973.

Wang, G., K. Kawamura, S. Lee, K. Ho, and J. Cao (2006), Molecular, seasonal, and spatial distributions of organic aerosols from fourteen Chinese cities, *Environ. Sci. Technol.*, *40*, 4619–4625, doi:10.1021/es060291x.

Wilkening, K. E., L. A. Barrie, and M. Engle (2000), Trans-Pacific air pollution, *Science*, *290*, 65–67, doi:10.1126/science.290.5489.65.

Winker, D. M., J. R. Pelon, and M. P. McCormick (2003), The CALIPSO mission: spaceborne lidar for observations of aerosols and clouds, *Proc. SPIE Int. Soc. Opt. Eng.*, *4893*, 1–11, doi:10.1117/12.466539.

Wotawa, G., and M. Trainer (2000), The influence of Canadian forest fires on pollutant concentrations in the United States, *Science*, *288*, 324–328, doi:10.1126/science.288.5464.324.

Wotawa, G., L.-E. De Geer, A. Bekcer, R. D'Amours, M. Jean, R. Servranckx, and K. Ungar (2006), Inter- and intra-continental transport of radioactive cesium released by boreal forest fires, *Geophys. Res. Lett.*, *33*, L12806, doi:10.1029/2006GL026206.

Xu, X., L. Wang, and T. Niu (1998), Air pollution and its health effects in Beijing, *Ecosyst. Health*, *4*, 199–209, doi:10.1046/j.1526-0992.1998.98096.x.

Yu, H., et al. (2003), Annual cycle of global distributions of aerosol optical depth from integration of MODIS retrievals and GOCART model simulations, *J. Geophys. Res.*, *108*(D3), 4128, doi:10.1029/2002JD002717.

Yu, H., et al. (2004), The direct radiative effect of aerosols as determined from a combination of MODIS retrievals and GOCART simulations, *J. Geophys. Res.*, *109*, D03206, doi:10.1029/2003JD003914.

Yu, H., et al. (2006), A review of measurement-based assessments of the aerosol direct radiative effect and forcing, *Atmos. Chem. Phys.*, *6*, 613–666.

Zhang, R., G. Li, J. Fan, D. L. Wu, and M. J. Molina (2007), Intensification of Pacific storm track linked to Asian pollution, *Proc. Natl. Acad. Sci. U. S. A.*, *104*(13), 5295–5299, doi:10.1073/pnas.0700618104.

H. Bian, M. Chin, T. Diehl, R. G. Kleidman, L. A. Remer, and H. Yu, NASA Goddard Space Flight Center, Code 613.2, Greenbelt, MD 20771, USA. (hongbin.yu@nasa.gov)